

Towards early dark energy and $n_s=1$ with Planck, ACT and SPT

Jun-Qian Jiang^a Yun-Song Piao^{a,b,c,d}

^a*School of Physics, University of Chinese Academy of Sciences, Beijing 100049, China*

^b*School of Fundamental Physics and Mathematical Sciences, Hangzhou Institute for Advanced Study, UCAS, Hangzhou 310024, China*

^c*International Center for Theoretical Physics Asia-Pacific, Beijing/Hangzhou, China*

^d*Institute of Theoretical Physics, Chinese Academy of Sciences, P.O. Box 2735, Beijing 100190, China*

E-mail: jqjiang@zju.edu.cn, yspiao@ucas.ac.cn

ABSTRACT: We investigate the constraints on early dark energy (EDE) by combining the most recent CMB observations available, ACT DR4, SPT-3G, and Planck2018 ($\ell_{\text{TT,max}} = 1000$) data. This combined CMB dataset favors non-zero EDE fractions and large Hubble constants, i.e. $H_0 = 72.3(73.4)_{-1.7}^{+2.2}$ and $73.32(72.98)_{-0.95}^{+0.68}$ km/s/Mpc for axion-like EDE and AdS-EDE, respectively. The inclusion of BAO+Pantheon data has little effect on the results. The axion-like EDE can fit the data significantly better ($\Delta\chi^2 \lesssim -10$) than Λ CDM, which is mainly driven by the ACT data. It is found again that if the current H_0 measured locally is correct, complete resolution of the Hubble tension seems to be pointing towards a scale invariant Harrison-Zeldovich spectrum of primordial scalar perturbation, i.e. $n_s = 1$ for $H_0 \sim 73$ km/s/Mpc.

Contents

1	Introduction	1
2	Model, Data and Methodology	2
3	Results	3
3.1	axion-like EDE	3
3.2	AdS-EDE	6
4	Discussion	7
4.1	Where do the differences in model fit come from?	7
4.2	Why does the high- ℓ part of Planck TT not favor the EDE model?	8
4.3	$n_s = 1$?	10
5	Conclusion	11

1 Introduction

As the precision of cosmological observations increases, the standard Λ CDM model is facing challenges. One of the critical problems is the $4 \sim 6\sigma$ tension between the Hubble constant based on the early universe with the Λ CDM model and that measured by direct observations of the local universe without assuming the Λ CDM model [1, 2] (see e.g. [3–5] for recent reviews), dubbed as the Hubble tension. The systematic errors are unable to explain it entirely, so modifications to the cosmological model is required.

Pre-recombination early dark energy (EDE) [6, 7] is one of the most promising route to resolve the Hubble tension. In corresponding scenario, energy injection before recombination led to faster expansion of the Universe, which so reduced the sound horizon. As $\theta_s^* = r_s^*/D_A^*$ is measured precisely by CMB observations, we can obtain a higher H_0 while keeping late-time physics unchanged. There are various kinds of phenomenological models [7–17] for this early energy injection with effective fluids or scalar fields, see also [18–20]. Decay of EDE must be rapid so as not to spoil other observations, which can be achieved by an oscillatory potential in axion-like EDE, e.g.Refs.[7, 8], or by an anti-de Sitter (AdS) phase in AdS-EDE [13]. Both showed a better fit to the CMB, baryon acoustic oscillation (BAO) and local H_0 data.

Planck data, the most precise large-scale CMB observation currently available, alone seems not favor axion-like EDE model (see Ref.[21]). However, the Planck data itself is debatable, especially its small scale part of TT power spectrum. The inconsistency between the $\ell < 1000$ and $\ell > 1000$ part of Planck’s TT power spectrum has been pointed out in Refs.[22, 23]. Moreover, the smoothing effect of gravitational lensing on acoustic peaks

of the CMB power spectrum exceeds that expected in Λ CDM model [22, 24]. However, ground-based CMB observations, such as ACT and SPT, providing precise measurements on small scale power spectrum have not found this over-smoothing effect [25–27].

It has been found that, without the small scale part of Planck TT power spectrum, a large fraction of EDE and a large Hubble constant are possible. Recently, combined analysis of Planck data ($\ell_{\text{TT}} \lesssim 1000$) with ACT or SPT data have been performed for EDE models, such as Planck + SPTpol for power-law potential EDE [28], axion-like EDE [29], AdS-EDE [30] and Planck + ACT DR4 for axion-like EDE [31, 32] and NEDE [32]. And also Planck + ACT DR4 + SPT-3G Y1 for axion-like EDE [33].

In this work, in view of the important role of ground-based CMB observations, we investigate the constraints on axion-like EDE and AdS-EDE models using the combination of Planck18 data (we exclude $\ell > 1000$ part of Planck TT power spectrum) with the recent SPT-3G Y1 and ACT DR4 data, with and without BAO and Pantheon data. We find that this combined CMB dataset favors a non-zero EDE fraction and a large Hubble constant for both models. In Ref.[34], it has been found that with fullPlanck+BAO+Pantheon dataset the pre-recombination solutions of the Hubble tension implies a scale-invariant Harrison-Zeldovich spectrum of primordial scalar perturbation, i.e. $n_s = 1$ for $H_0 \sim 73$ km/s/Mpc. It is also interesting to recheck this conclusion with our combined CMB dataset.

The paper is outlined as follows. We explain our data, models and methodology in section 2. Results are presented in section 3. Then we analyse and discuss it in section 4. Finally, we conclude in section 5.

2 Model, Data and Methodology

The first EDE model is: axion-like EDE, where the energy injection before recombination is achieved by a scale field with axion-like potential [7]:

$$V(\phi) = m^2 f^2 (1 - \cos \theta)^n, \text{ where } \theta = \phi/f \in [-\pi, \pi] \quad (2.1)$$

It describes the axion for $n = 1$, which naturally arises in high energy theory. Initially, the field sit in the upper region of its potential due to the Hubble friction, resulted in $w \approx -1$, i.e. an dark energy injection. Afterwards it will roll to the bottom of the potential and oscillate with $w \approx (n - 1)/(n + 1)$. Therefore, the energy will redshift faster than matter if $n > 1$, avoid degrading other measurements (e.g. matter density and CMB). Here, we fixed $n = 3$, which is a suitable value for the current data [8].

Another model we consider is AdS-EDE, with phenomenological potential [13, 30]: ¹

$$V(\phi) = \begin{cases} V_0 \left(\frac{\phi}{M_{\text{Pl}}} \right)^4 - V_{\text{AdS}}, & \frac{\phi}{M_{\text{Pl}}} < \left(\frac{V_{\text{AdS}}}{V_0} \right)^{1/4} \\ 0, & \frac{\phi}{M_{\text{Pl}}} > \left(\frac{V_{\text{AdS}}}{V_0} \right)^{1/4} \end{cases} \quad (2.2)$$

where M_{Pl} is the reduced Planck mass. V_{AdS} is the depth of AdS phase. The significant difference from axion-like EDE is that the energy redshifts in an AdS phase. In an AdS

¹Other potentials are also possible [35].

phase with $w > 1$ the energy of EDE can redshift faster than that in oscillation phase, thus results less destruction to other measurement.² It is well-known that AdS vacua is ubiquitous in high energy theories, so the AdS-EDE model can be well-motivated, see also the applications of AdS vacua to late Universe [36–42].

We consider the following CMB data sets at first:

- **Planck 2018:** We use the low- ℓ TT,EE **Commander** likelihoods and high- ℓ TT,TE,EE **Plik** likelihoods, with also the reconstructed lensing power spectrum [43].
- **SPT-3G Y1:** We use the public SPT-3G likelihood³, which includes TE and EE power spectrum within multipoles $300 < \ell < 3000$ [27].
- **ACT DR4:** We use the marginalized likelihood⁴ from ACT Data Release 4, which includes TE and EE power spectrum within multipoles $326 < \ell < 4325$ and TT power spectrum within multipoles $576 < \ell < 4325$ [44].

This data set combination is confirmed in Ref.[45], which showed $H_0 = 67.49 \pm 0.53$ km/s/Mpc for Λ CDM model. As mentioned, it might be better to discard the small scale part of Planck’s TT, so when combine Planck measurement with ACT and SPT data, we cut the Planck’s high- ℓ TT power spectrum to $\ell_{\text{TT,max}} = 1000$.⁵ Then, we use galaxy BAO measurements from 6DF [46], SDSS DR7 MGS [47] in low- z and BOSS DR12 [48] in high- z . Type Ia supernovae from Pantheon [49] is also used.

We perform MCMC sampling with **Cobaya** [50]. The models are calculated using the modified **CLASS** [51]⁶, where we improved the accuracy for the calculation of the lensing effect since it has non-negligible effects on the small-scale CMB power spectrum. The Gelman-Rubin criterion for all chains is converged to $R - 1 < 0.1$.

Here, we adopt same parameters and priors as Refs.[32] and [30], for axion-like EDE model: $\log_{10}(z_c) \in [2, 4.5]$, $f_{\text{EDE}} \in [0, 0.3]$, where z_c is the redshift at which the field starts rolling and f_{EDE} is the energy fraction of EDE at z_c , the initial position of EDE field $\Theta_{\text{ini}} \in [0, 3.1]$, while for AdS-EDE model: $\ln(1 + z_c) \in [7.5, 9]$, $f_{\text{EDE}} \in [0, 0.3]$. In order to have a significant AdS phase while make the field able to climb out of the AdS well, we fixed $\alpha_{\text{AdS}} \equiv (\rho_{\text{m}}(z_c) + \rho_{\text{r}}(z_c)) / V_{\text{AdS}} = 3.79 \times 10^{-4}$ as [13]. The neutrino assumption is the same as Planck [43]. The posterior distribution is plotted using **GetDist** [52].

3 Results

3.1 axion-like EDE

We show the posterior distribution in **Figure 1** and the mean (best-fit) values of cosmological parameters in **Table 1**. The result is similar to Refs.[54] with $\ell_{\text{TT,max}} = 650$, where BAO

²The difference between the power-law and cosine potentials in the axion EDE is also important [8].

³https://github.com/SouthPoleTelescope/spt3g_y1_dist

⁴<https://github.com/ACTCollaboration/pyactlike>

⁵This choice of $\ell_{\text{TT,max}}$ is the same as Refs.[28–30] and close to Refs.[32] (where $\ell_{\text{TT,max}} = 1060$) and [31, 33] (where $\ell_{\text{TT,max}} = 650$).

⁶The codes are available at <https://github.com/PoulinV/AxiCLASS> for axion-like EDE and https://github.com/genye00/class_multiscf for AdS-EDE.

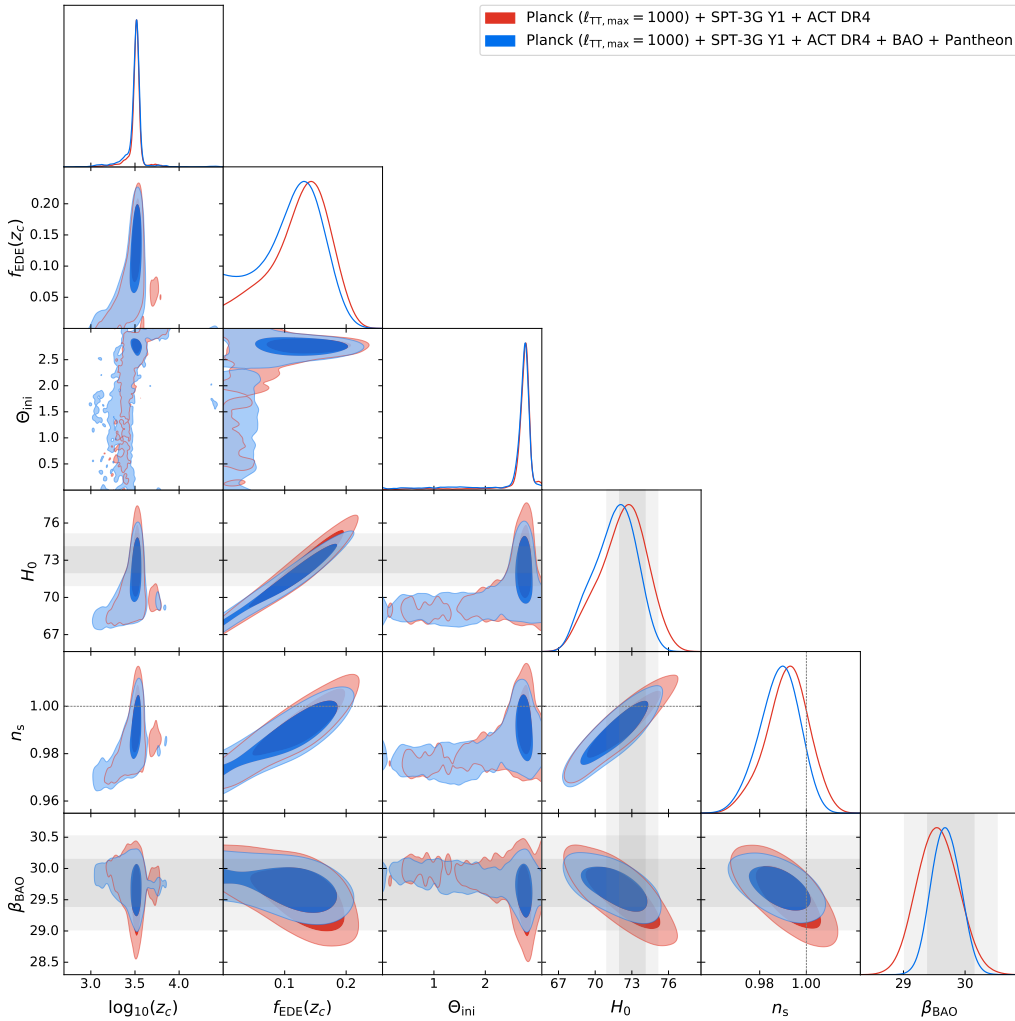


Figure 1. Posterior distributions of relevant parameters in axion-like EDE model (68% and 95% confidence range). Grey bands represent the 1σ and 2σ regions of the SH0ES measurement [53] and model-independent constraint on β_{BAO} from BAO and SN, respectively.

and SN data were not included. We see that Planck($\ell_{\text{TT}, \text{max}} = 1000$)+ACT DR4+SPT-3G Y1 dataset alone favor a non-zero fraction of EDE $f_{\text{EDE}} = 0.124(0.168)_{-0.034}^{+0.060}$ and a large Hubble constant $H_0 = 72.3(73.4)_{-1.7}^{+2.2}$, which is compatible with the SH0ES result [53].

The inclusion of BAO+Pantheon does not alter the result too much. This can be confirmed by checking $\beta_{\text{BAO}} \equiv c / (H r_s^{\text{darg}})$, which BAO+Pantheon mainly constrain. We can find in Figure 1 that the β_{BAO} obtained from CMB data alone is consistent with that constrained by BAO+SN observations.⁷ Besides, the preference for large Θ_{ini} due to the inclusion of Planck’s high- ℓ TE,EE power spectrum, is in agreement with the analysis in [8]. Unlike Ref.[31], we find $\log_{10}(z_c) \approx 3.5$, close to the matter-radiation equality, even with lensing and BAO data included. This is because a larger Θ_{ini} prefers the parameter

⁷BAO+Pantheon constraints on β_{BAO} are calculated in [30] based on the model-independent approach described in [55, 56].

parameters	Planck($\ell_{\text{TT, max}} = 1000$) +ACT DR4+SPT-3G Y1	Planck($\ell_{\text{TT, max}} = 1000$) +ACT DR4+SPT-3G Y1 +BAO+Pantheon	Planck +BAO+Pantheon
f_{EDE}	0.124(0.150) $^{+0.060}_{-0.034}$	0.111(0.148) $^{+0.063}_{-0.037}$	< 0.084(0.09)
$\log_{10}(z_c)$	3.505(3.514) $^{+0.048}_{-0.024}$	3.497(3.521) $^{+0.062}_{-0.025}$	unconstrained (3.569)
Θ_{ini}	2.64(2.80) $^{+0.23}_{+0.029}$	2.53(2.75) $^{+0.34}_{+0.11}$	1.933(2.773) $^{+1.2}_{-0.44}$
H_0	72.3(73.4) $^{+2.2}_{-1.7}$	71.6(72.9) $^{+2.0}_{-1.5}$	68.6(70.88) $^{+0.55}_{-1.1}$
$100\omega_b$	2.263(2.262) $^{+0.017}_{-0.019}$	2.259(2.267) $^{+0.017}_{-0.019}$	2.257(2.270) $^{+0.017}_{-0.02}$
ω_{cdm}	0.1316(0.1340) $^{+0.0065}_{-0.0049}$	0.1306(0.1348) $^{+0.0067}_{-0.0053}$	0.1219(0.1278) $^{+0.0013}_{-0.0034}$
$10^9 A_s$	2.138(2.141) \pm 0.034	2.126(2.140) \pm 0.035	2.118(2.159) $^{+0.031}_{-0.034}$
n_s	0.9918(0.9962) $^{+0.0099}_{-0.0083}$	0.9884(0.9933) $^{+0.0094}_{-0.0078}$	0.9719(0.9850) $^{+0.0048}_{-0.0076}$
τ_{reio}	0.0531(0.0526) \pm 0.0072	0.0510(0.0516) $^{+0.0078}_{-0.0069}$	0.0569(0.0617) $^{+0.0071}_{-0.0078}$
S_8	0.832(0.830) \pm 0.014	0.833(0.839) \pm 0.014	0.828(0.836) \pm 0.013
Ω_m	0.2967(0.2921) \pm 0.0085	0.3000(0.2975) \pm 0.0059	0.3085(0.3008) \pm 0.0059

Table 1. The mean (best-fit) $\pm 1\sigma$ errors of parameters in axion-like EDE model for each dataset combination, The result with fullPlanck+BAO+Pantheon is from Ref.[32].

parameters	Planck($\ell_{\text{TT, max}} = 1000$) +ACT DR4+SPT-3G Y1	Planck($\ell_{\text{TT, max}} = 1000$) +ACT DR4+SPT-3G Y1 +BAO+Pantheon	Planck +BAO+Pantheon
f_{EDE}	0.1258(0.1199) $^{+0.0051}_{-0.014}$	0.1257(0.1163) $^{+0.0050}_{-0.014}$	0.1124(0.1084) $^{+0.0038}_{-0.0070}$
$\ln(1 + z_c)$	8.009(8.007) $^{+0.061}_{-0.075}$	8.012(7.968) $^{+0.063}_{-0.072}$	8.153(8.147) $^{+0.075}_{-0.084}$
H_0	73.32(72.98) $^{+0.68}_{-0.95}$	73.17(72.74) $^{+0.56}_{-0.80}$	72.52(72.46) \pm 0.51
$100\omega_b$	2.309(2.311) \pm 0.022	2.308(2.299) \pm 0.020	2.341(2.331) $^{+0.018}_{-0.016}$
ω_{cdm}	0.1367(0.1361) $^{+0.0022}_{-0.0028}$	0.1371(0.1358) $^{+0.0016}_{-0.0027}$	0.1346(0.1336) $^{+0.0016}_{-0.0018}$
$10^9 A_s$	2.134(2.138) $^{+0.040}_{-0.033}$	2.132(2.120) $^{+0.035}_{-0.031}$	2.175(2.159) \pm 0.033
n_s	1.0013(1.0021) \pm 0.0068	1.0014(0.9989) $^{+0.0056}_{-0.0064}$	0.9964(0.9949) $^{+0.0047}_{-0.0041}$
τ_{reio}	0.0453(0.0468) $^{+0.010}_{-0.0083}$	0.0445(0.0433) $^{+0.0090}_{-0.0076}$	0.0545(0.0523) $^{+0.0071}_{-0.0079}$
S_8	0.857(0.860) \pm 0.018	0.861(0.858) \pm 0.012	0.863(0.856) \pm 0.011
Ω_m	0.2987(0.3001) \pm 0.0090	0.3004(0.3014) \pm 0.0061	0.3016(0.3002) \pm 0.0051

Table 2. The mean (best-fit) $\pm 1\sigma$ errors of parameters in AdS-EDE model for each dataset combination, The result with fullPlanck+BAO+Pantheon is from Ref.[30].

region with smaller z_c , which can also be found in the Appendix B of Ref.[32].

We present the χ^2 for the bestfit points in Table 3 and Table 4. We found significant improvements $\Delta\chi^2 \approx -11$ without and with BAO+Pantheon for axion-like EDE model compared to Λ CDM in fitting CMB data. The main improvement is come from CMB data, especially ACT DR4 and Planck high- ℓ part.

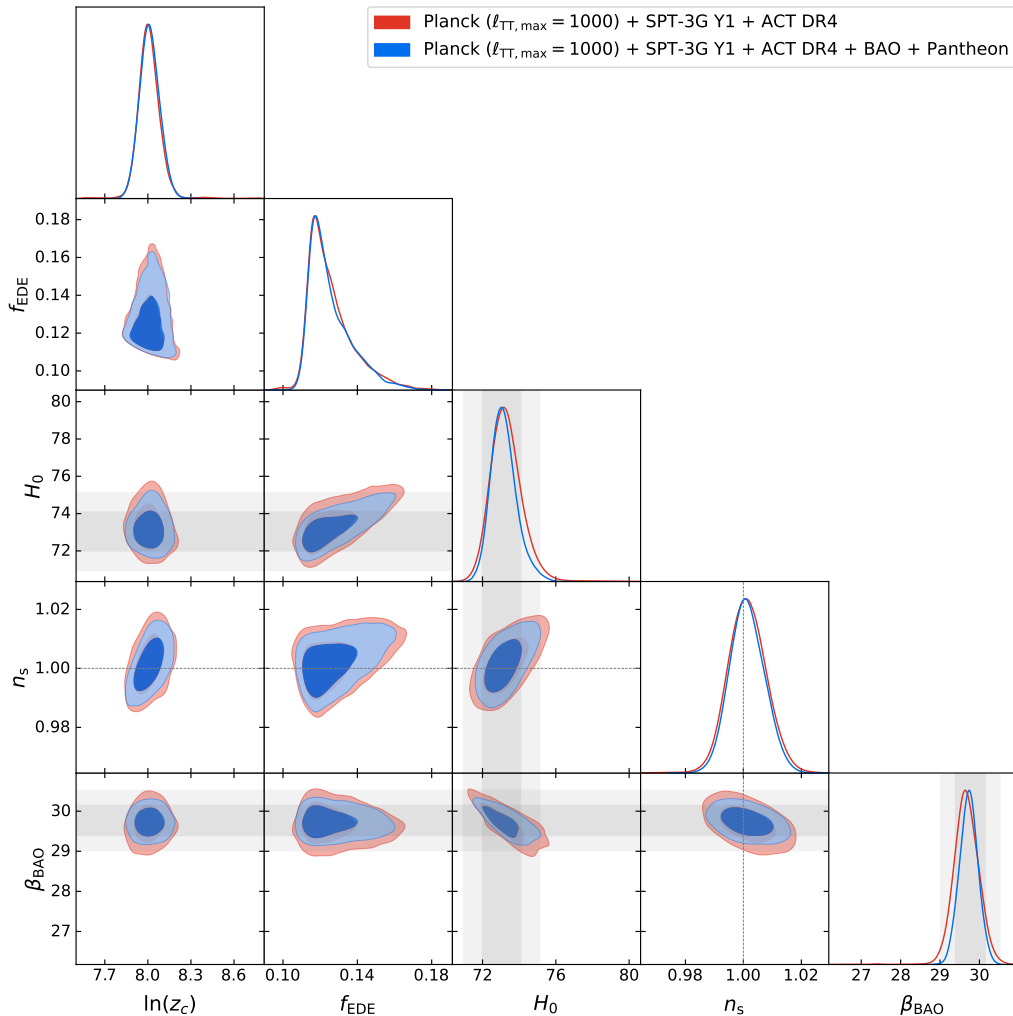


Figure 2. Posterior distributions of relevant parameters in AdS-EDE model (68% and 95% confidence range). Grey bands represent the 1σ and 2σ regions of the SHOES measurement [53] and model-independent constraint on β_{BAO} from BAO and SN, respectively.

3.2 AdS-EDE

The combined CMB dataset still favor a non-zero fraction of AdS-EDE $f_{\text{EDE}} = 0.1258(0.1199)^{+0.0051}_{-0.014}$ and a large Hubble constant $H_0 = 73.32(72.98)^{+0.68}_{-0.95}$, see the posterior distribution in Figure 2 and the mean (best-fit) values in Table 2, and the inclusion of BAO+Pantheon does not change the results. However, different from that for axion-like EDE, the fullPlanck+BAO+Pantheon dataset still favor a large $H_0 = 72.52(72.46) \pm 0.51$ for AdS-EDE. A distinct non-Gaussian distribution is shown in $f_{\text{EDE}}\text{-}\ln(z_c)$ plane. This is a reflection of AdS bound, or else the EDE field will be unable to climb out of AdS well.

We present the χ^2 for the bestfit points in Table 3 and Table 4. We find that AdS-EDE shows about $\Delta\chi^2 \approx +2$ worse fit to the corresponding dataset than ΛCDM , mainly comes from Planck lensing. This difference is statistically insignificant. However, similar to ΛCDM , AdS-EDE does not fit better to Planck high- ℓ part and ACT data, compared with

axion-like EDE. Here, we only have investigated the simplest AdS-EDE model, actually other AdS potentials are also possible. Note that the bestfit point is so close to AdS bound that the “real” bestfit point might be covered by it. The AdS bound is controlled by α_{AdS} , thus a smaller α_{AdS} can bring a better fit.

	ΛCDM	axion-like EDE	AdS-EDE
Planck low- ℓ TT	21.74	20.63	20.32
Planck low- ℓ EE	395.72	395.83	396.21
Planck high- ℓ TTTEE ($\ell_{\text{TT, max}} = 1000$)	1985.91	1983.32	1982.90
Planck lensing	9.16	10.73	11.32
ACT DR4	297.48	289.17	300.03
SPT-3G Y1	1117.31	1116.94	1118.93
total χ^2	3827.32	3816.61	3829.72
$\chi^2_{\text{model}-\Lambda\text{CDM}}$		-10.71	+2.40

Table 3. χ^2 values for best-fit models to Planck ($\ell_{\text{TT, max}} = 1000$) + ACT DR4 + SPT-3G Y1 dataset.

	ΛCDM	axion-like EDE	AdS-EDE
Planck low- ℓ TT	21.54	20.81	20.45
Planck low- ℓ EE	396.11	395.84	395.85
Planck high- ℓ TTTEE ($\ell_{\text{TT, max}} = 1000$)	1986.18	1981.81	1984.92
Planck lensing	9.27	10.41	11.20
ACT DR4	297.60	290.54	297.92
SPT-3G Y1	1117.60	1117.01	1118.44
BAO low- z	1.67	2.25	1.86
BOSS DR12 BAO	3.57	3.50	3.50
Pantheon	1034.81	1034.74	1034.75
total χ^2	4868.34	4856.90	4869.91
$\chi^2_{\text{model}-\Lambda\text{CDM}}$		-11.44	+1.57

Table 4. χ^2 values for best-fit models to Planck ($\ell_{\text{TT, max}} = 1000$) + ACT DR4 + SPT-3G Y1 + BAO + Pantheon dataset.

4 Discussion

4.1 Where do the differences in model fit come from?

As the main improvements come from the ACT and Planck high- ℓ part, we display the cumulative $\Delta\chi^2$ of them in [Figure 3](#) to clarify the origin of the data in favor of the axion-like EDE model. It is clear that the preference for the axion-like EDE arises mainly from the narrow $\ell \approx 1300$ part of the ACT TE spectrum and the wide $1400 \lesssim \ell \lesssim 2000$ part of the ACT TT spectrum, where the latter is also valid for AdS-EDE. The lowest several bins of the ACT EE spectrum also contribute to the improvement for both model (similar

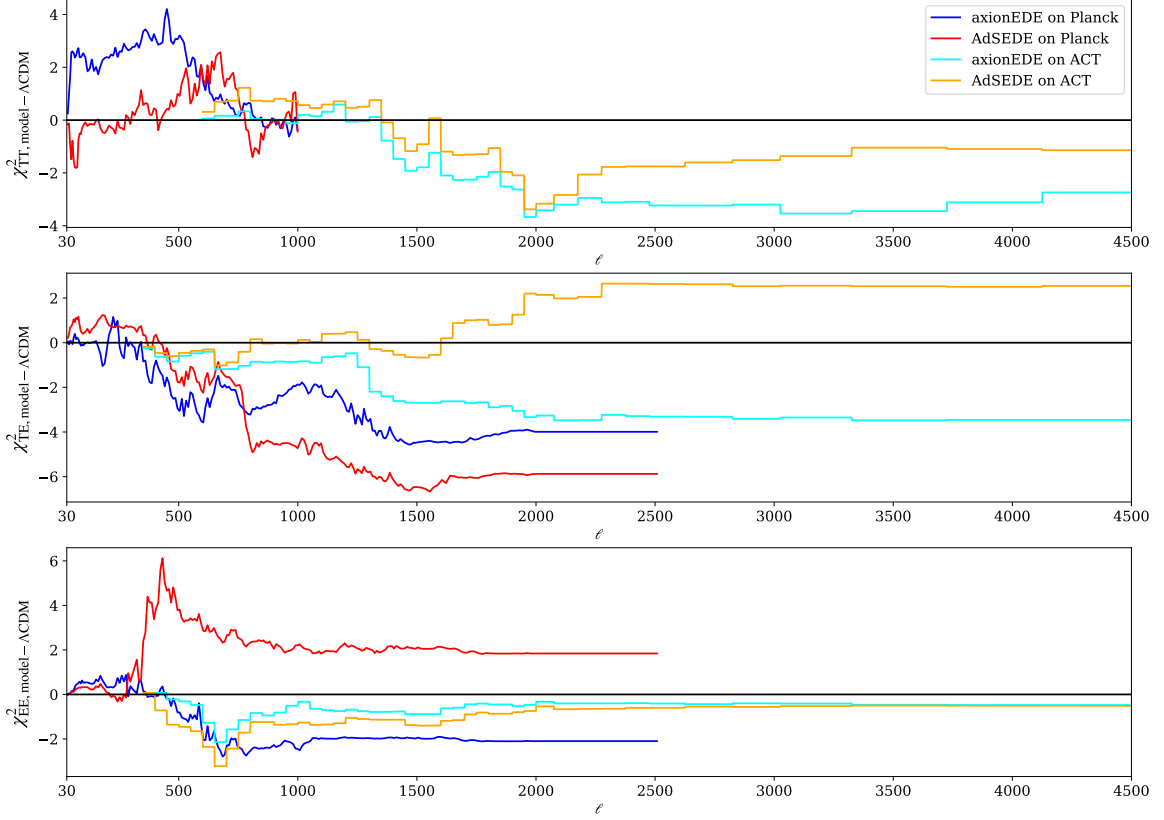


Figure 3. The cumulative $\chi^2_{\text{model}-\Lambda\text{CDM}}$ of each part of data in the best-fit points to Planck ($\ell_{\text{TT, max}} = 1000$) + ACT DR4 + SPT-3G Y1 + BAO + Pantheon.

to the analysis in [31]). However, the next few bins could not be fitted well, resulting in no significant preference in the ACT EE spectrum.

The exact reasons can be found in the residual plots (Figure 4). ACT data in the $\ell \approx 1300$ part of the TE spectrum seems to favor smaller values, and the axion-like EDE captures this point. Besides, in the axion-like EDE model, there seems to be a shift to larger ℓ since the 5th acoustic peak of the TT spectrum. This shift is more visible in the EE spectrum.

In addition, the axion-like EDE model also provides a better fit to the $\ell \lesssim 900$ part of Planck TE,EE spectrum. Some of them come from the previously mentioned shift toward high ℓ .

4.2 Why does the high- ℓ part of Planck TT not favor the EDE model?

There are some oscillatory residuals in the Planck TT high- ℓ part, and such oscillatory residuals might be related to the lensing anomaly [22, 24] and parameter differences between different scales of the Planck TT spectrum [22, 23]. Although oscillatory residuals also appear in our bestfit EDE model, it is in a different phase than the oscillatory residuals of the high- ℓ part of Planck TT spectrum, see Figure 4.

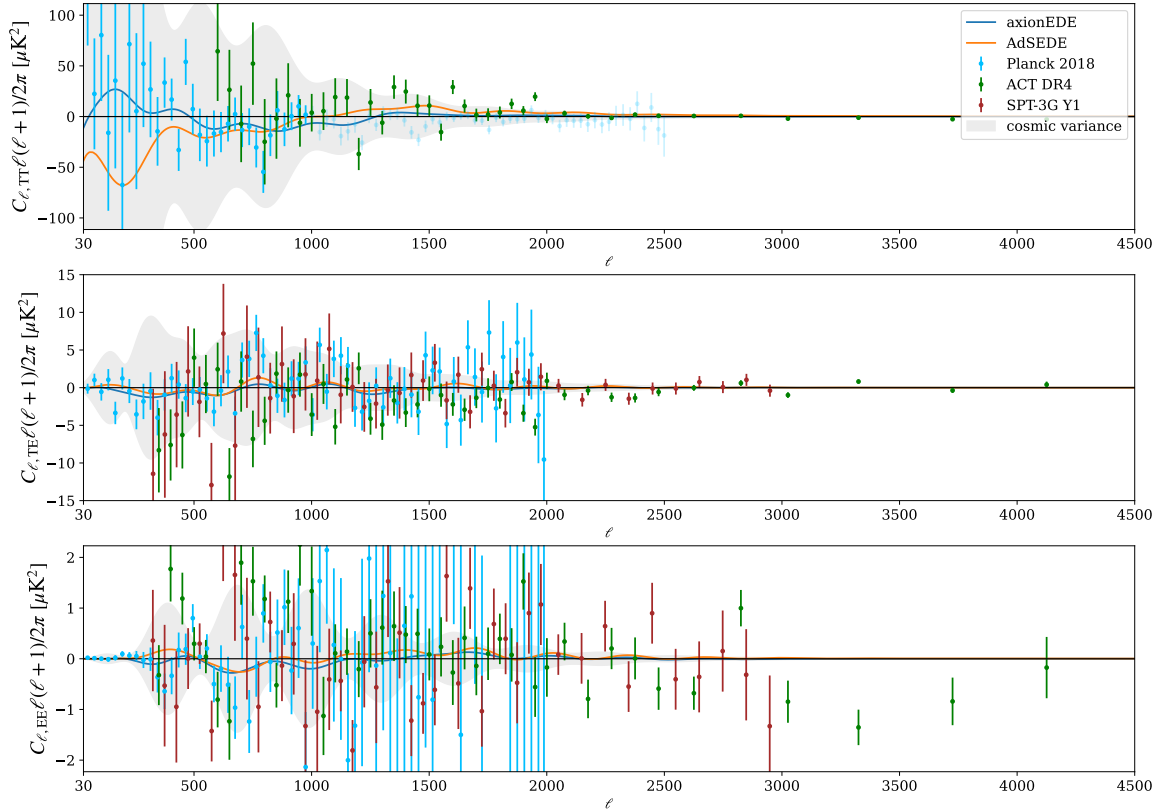


Figure 4. The residuals of the best-fit points for each model relative to Λ CDM model in Planck ($\ell_{\text{TT, max}} = 1000$) + ACT DR4 + SPT-3G Y1 + BAO + Pantheon and the constraints of different CMB data. The light colored part of the Planck TT spectrum is the unused data.

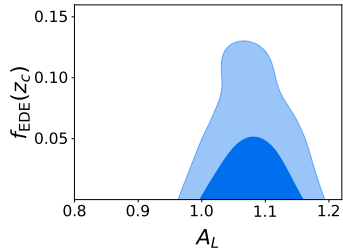


Figure 5. The relation between A_L and f_{EDE} in axion-like EDE model with fullPlanck + BAO + Pantheon dataset.

Nevertheless, we considered the simplest possibility: whether the possible solution to the lensing anomaly is related to that the high- ℓ part of Planck TT spectrum disfavors the EDE models? We performed the MCMC analysis by varying the rescaling factor A_L (see [57] for standard definition) of the lensing potential with the fullPlanck+BAO+Pantheon dataset. The results are presented in Figure 5, where we do not find any significant degeneracy between A_L and EDE parameters, which suggests that the lensing anomaly alone cannot explain this disfavor to EDE models. See Fig.6 in [58] for an attempt to modify

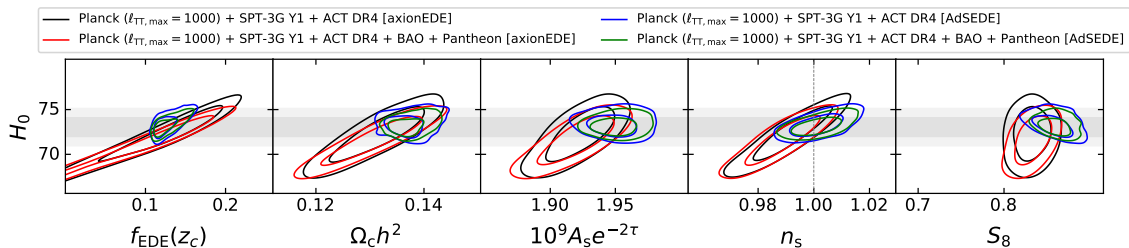


Figure 6. The degeneracy between parameters under different models and datasets.

late dark energy.

However, it is important to note that the lensing anomaly is only a naive reflection of the oscillation pattern on this Planck TT spectrum. In fact, lensing anomaly also cannot explain the inconsistency between different scales of the Planck TT spectrum [23]. And this oscillation pattern was not found in ground-based CMB observations (see also [14]), which can already be better than Planck constraints in $\ell \gtrsim 2000$, so further observations of the TT spectrum in the $1000 \lesssim \ell \lesssim 2000$ part are necessary.

4.3 $n_s = 1$?

In EDE models, some other cosmological parameters must be shifted to compensate the raising of H_0 . We show clear shifts of relevant parameters in Figure 6. As these parameters are shifted, the CMB power spectrum barely changes over the range of scales we are interested in, as showed by the black line in the Figure 7. This indicates that our CMB dataset is well constrained to the power spectrum.

In addition to altering r_s^* , pre-recombination EDE also affects the amplitude of power spectrum. Here, the Weyl potential will accelerated decay (eventually to a smaller level), as shown in Figure 8, see also [10, 59] for other EDE models. The faster decay of the Weyl potential results in the enhancement of CMB power spectrum of $\ell \lesssim 700$, which further leads to the enhancement of early ISW effect. In order to balance the enhancement of the early ISW effect, which is measured to be self-consistent in the Λ CDM model [60], ω_{cdm} is shifted to a larger value. The direction of shift is consistent with the constraint of BAO+Pantheon. The remaining power spectrum amplitude changes, especially around the pivot, is complemented by the overall amplitude $A_s e^{-2\tau}$.

The high ℓ part of power spectrum is mainly controlled by diffusion damping. The energy injection before recombination will amplify the ratio r_d/r_s^* , thus enhancing the damping as θ_s is well fixed. This can not be complemented fully by the rise of $A_s e^{-2\tau}$, leads to the rise of n_s , as shown in Figure 6.⁸

Actually, we have

$$\delta n_s \approx 0.3 \frac{\delta H_0}{H_0} \quad (4.1)$$

⁸The rises of n_s and ω_m result in a larger S_8 , which, however, can be lowered by new physics beyond cold dark matter [61–65], see also [66–68].

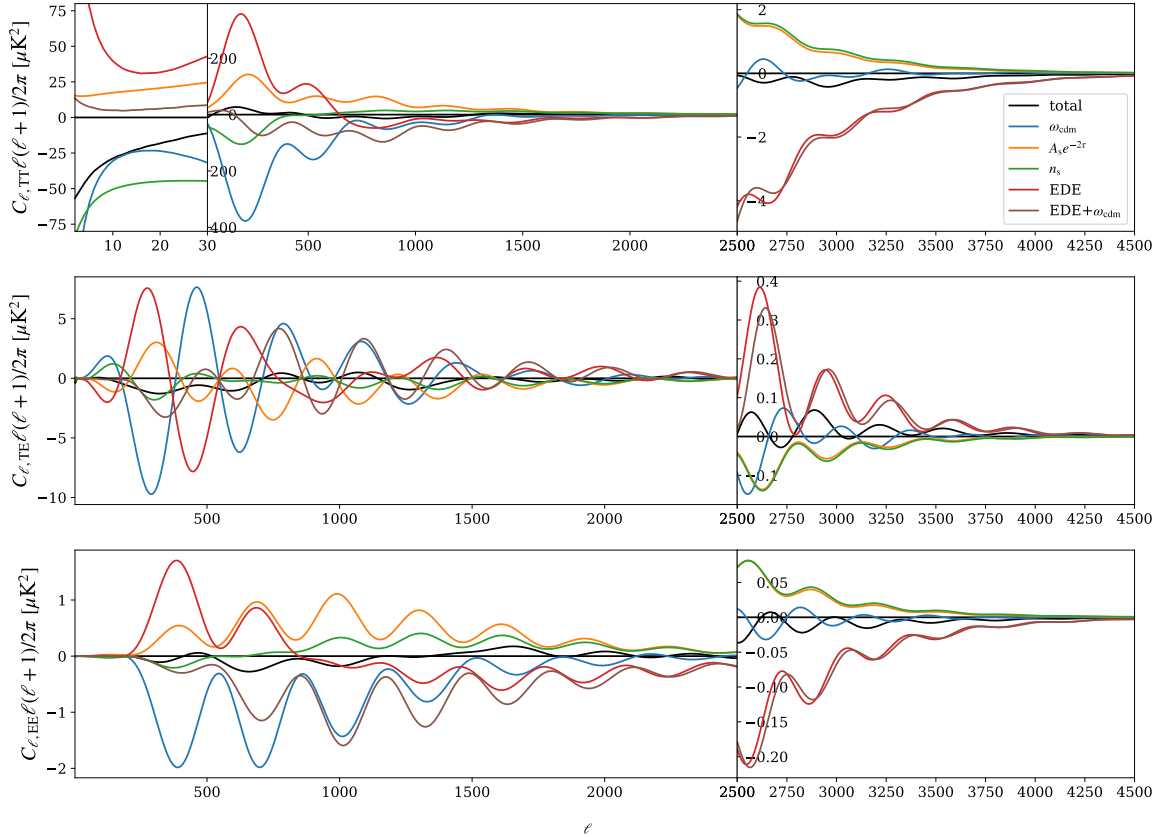


Figure 7. Relative changes in CMB power spectrum with respect to our bestfit Λ CDM model when changing certain parameters from Λ CDM to axion-like EDE bestfit values. θ_s^* is fixed by adjusting H_0 when changing ω_m and relevant EDE parameters.

for our combined CMB dataset, which is slightly different for other dataset, e.g. $\delta n_s \approx 0.4 \frac{\delta H_0}{H_0}$ for fullPlanck+BAO+Pantheon dataset [34], see also recent [69]. This is due to the different constraining power of the CMB datasets, especially in the region of diffusion damping. However, they all suggest $n_s = 1$, i.e. a scale invariant spectrum. This hints that the primordial Universe model might need to be reconsidered, e.g. [70, 71].

5 Conclusion

We investigated the constraints on EDE by combining the most precise CMB data available, i.e. Planck, SPT and ACT data. However, since the small scale part of Planck TT spectrum suffers from some anomalies, we exclude $\ell > 1000$ part of Planck TT power spectrum. Our main conclusions are as follows:

- The combined CMB dataset favors non-zero EDE fractions and large Hubble constants for both axion-like EDE and AdS-EDE models, i.e. $H_0 = 72.3(73.4)_{-1.7}^{+2.2}$ km/s/Mpc and $73.32(72.98)_{-0.95}^{+0.68}$ km/s/Mpc, respectively. The inclusion of BAO+Pantheon data does not change the results, i.e. $H_0 = 71.6(72.9)_{-1.5}^{+2.0}$ km/s/Mpc and $73.17(72.74)_{-0.80}^{+0.56}$,

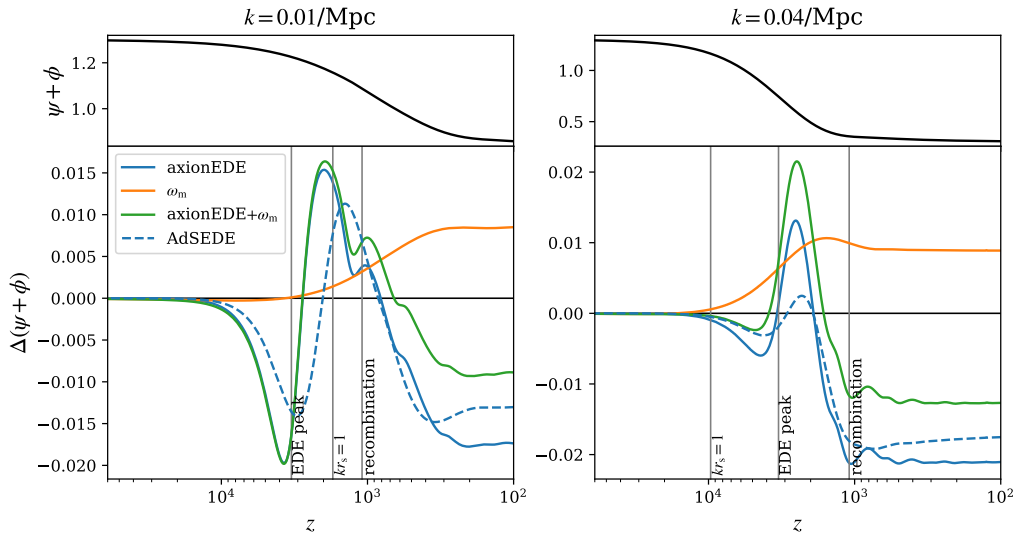


Figure 8. Relative changes in Weyl potential with respect to our bestfit Λ CDM model when changing certain parameters from Λ CDM to EDE bestfit values.

respectively. In addition, it is also noted that the fullPlanck+BAO+Pantheon dataset still favors a large $H_0 = 72.52(72.46) \pm 0.51$ km/s/Mpc for AdS-EDE.

- The axion-like EDE model can fit the data significantly better than Λ CDM, which is mainly driven by the ACT part.
- The reason for the disfavor of the high- ℓ part of Planck TT to EDE is that the oscillatory pattern of high- ℓ TT spectrum in EDE do not match the oscillatory residual of Planck. The lensing anomaly can not explain it.
- The scale relationship between n_s and H_0 reappears, see (Equation 4.1), which implies $n_s = 1$ for $H_0 \sim 73$ km/s/Mpc.

In fact, the first year result of SPT-3G only made use of half of a observing season and part of detectors [27], and also the results of ACT DR5 is being released [72]. Ground-based CMB observations will have even better constraints, which will help to reveal whether and how the CMB observations really favor the EDE models.

Note added: When this project will be completed, Ref.[73] is present, which has investigated the constraints on (axion-like) EDE using ACT DR4, SPT-3G, and Planck2018 ($\ell_{\text{TT}} < 650$) data, with and without BAO+Pantheon data.

Acknowledgments

We thank Gen Ye for helpful discussions. This work is supported by the NSFC, No.12075246, the KRPCAS, No.XDPB15. We acknowledge the Tianhe-2 supercomputer for providing computing resources.

References

- [1] L. Verde, T. Treu, and A. G. Riess, *Tensions between the Early and the Late Universe*, Nature Astron. **3** (7, 2019) 891, [[arXiv:1907.10625](#)].
- [2] A. G. Riess, *The Expansion of the Universe is Faster than Expected*, Nature Rev. Phys. **2** (2019), no. 1 10–12, [[arXiv:2001.03624](#)].
- [3] E. Di Valentino et al., *Snowmass2021 - Letter of interest cosmology intertwined II: The hubble constant tension*, Astropart. Phys. **131** (2021) 102605, [[arXiv:2008.11284](#)].
- [4] E. Di Valentino, O. Mena, S. Pan, L. Visinelli, W. Yang, A. Melchiorri, D. F. Mota, A. G. Riess, and J. Silk, *In the realm of the Hubble tension—a review of solutions*, Class. Quant. Grav. **38** (2021), no. 15 153001, [[arXiv:2103.01183](#)].
- [5] L. Perivolaropoulos and F. Skara, *Challenges for Λ CDM: An update*, [[arXiv:2105.05208](#)].
- [6] T. Karwal and M. Kamionkowski, *Dark energy at early times, the Hubble parameter, and the string axiverse*, Phys. Rev. D **94** (2016), no. 10 103523, [[arXiv:1608.01309](#)].
- [7] V. Poulin, T. L. Smith, T. Karwal, and M. Kamionkowski, *Early Dark Energy Can Resolve The Hubble Tension*, Phys. Rev. Lett. **122** (2019), no. 22 221301, [[arXiv:1811.04083](#)].
- [8] T. L. Smith, V. Poulin, and M. A. Amin, *Oscillating scalar fields and the Hubble tension: a resolution with novel signatures*, Phys. Rev. D **101** (2020), no. 6 063523, [[arXiv:1908.06995](#)].
- [9] P. Agrawal, F.-Y. Cyr-Racine, D. Pinner, and L. Randall, *Rock 'n' Roll Solutions to the Hubble Tension*, [[arXiv:1904.01016](#)].
- [10] M.-X. Lin, G. Benevento, W. Hu, and M. Raveri, *Acoustic Dark Energy: Potential Conversion of the Hubble Tension*, Phys. Rev. D **100** (2019), no. 6 063542, [[arXiv:1905.12618](#)].
- [11] J. Sakstein and M. Trodden, *Early Dark Energy from Massive Neutrinos as a Natural Resolution of the Hubble Tension*, Phys. Rev. Lett. **124** (2020), no. 16 161301, [[arXiv:1911.11760](#)].
- [12] F. Niedermann and M. S. Sloth, *New early dark energy*, Phys. Rev. D **103** (2021), no. 4 L041303, [[arXiv:1910.10739](#)].
- [13] G. Ye and Y.-S. Piao, *Is the Hubble tension a hint of AdS phase around recombination?*, Phys. Rev. D **101** (2020), no. 8 083507, [[arXiv:2001.02451](#)].
- [14] M.-X. Lin, W. Hu, and M. Raveri, *Testing H_0 in Acoustic Dark Energy with Planck and ACT Polarization*, Phys. Rev. D **102** (2020) 123523, [[arXiv:2009.08974](#)].
- [15] M. Braglia, W. T. Emond, F. Finelli, A. E. Gumrukcuoglu, and K. Koyama, *Unified framework for early dark energy from α -attractors*, Phys. Rev. D **102** (2020), no. 8 083513, [[arXiv:2005.14053](#)].
- [16] S. Nojiri, S. D. Odintsov, D. Saez-Chillon Gomez, and G. S. Sharov, *Modeling and testing the equation of state for (Early) dark energy*, Phys. Dark Univ. **32** (2021) 100837, [[arXiv:2103.05304](#)].
- [17] T. Karwal, M. Raveri, B. Jain, J. Khoury, and M. Trodden, *Chameleon Early Dark Energy and the Hubble Tension*, [[arXiv:2106.13290](#)].

- [18] M. Zumalacarregui, *Gravity in the Era of Equality: Towards solutions to the Hubble problem without fine-tuned initial conditions*, Phys. Rev. D **102** (2020), no. 2 023523, [[arXiv:2003.06396](#)].
- [19] G. Ballesteros, A. Notari, and F. Rompineve, *The H_0 tension: ΔG_N vs. ΔN_{eff}* , JCAP **11** (2020) 024, [[arXiv:2004.05049](#)].
- [20] M. Braglia, M. Ballardini, F. Finelli, and K. Koyama, *Early modified gravity in light of the H_0 tension and LSS data*, Phys. Rev. D **103** (2021), no. 4 043528, [[arXiv:2011.12934](#)].
- [21] J. C. Hill, E. McDonough, M. W. Toomey, and S. Alexander, *Early dark energy does not restore cosmological concordance*, Phys. Rev. D **102** (2020), no. 4 043507, [[arXiv:2003.07355](#)].
- [22] G. E. Addison, Y. Huang, D. J. Watts, C. L. Bennett, M. Halpern, G. Hinshaw, and J. L. Weiland, *Quantifying discordance in the 2015 Planck CMB spectrum*, Astrophys. J. **818** (2016), no. 2 132, [[arXiv:1511.00055](#)].
- [23] **Planck** Collaboration, N. Aghanim et al., *Planck intermediate results. LI. Features in the cosmic microwave background temperature power spectrum and shifts in cosmological parameters*, Astron. Astrophys. **607** (2017) A95, [[arXiv:1608.02487](#)].
- [24] P. Motloch and W. Hu, *Lensinglike tensions in the Planck legacy release*, Phys. Rev. D **101** (2020), no. 8 083515, [[arXiv:1912.06601](#)].
- [25] **SPT** Collaboration, J. W. Henning et al., *Measurements of the Temperature and E-Mode Polarization of the CMB from 500 Square Degrees of SPTpol Data*, Astrophys. J. **852** (2018), no. 2 97, [[arXiv:1707.09353](#)].
- [26] **ACT** Collaboration, S. Aiola et al., *The Atacama Cosmology Telescope: DR4 Maps and Cosmological Parameters*, JCAP **12** (2020) 047, [[arXiv:2007.07288](#)].
- [27] **SPT-3G** Collaboration, D. Dutcher et al., *Measurements of the E-mode polarization and temperature-E-mode correlation of the CMB from SPT-3G 2018 data*, Phys. Rev. D **104** (2021), no. 2 022003, [[arXiv:2101.01684](#)].
- [28] A. Chudaykin, D. Gorbunov, and N. Nedelko, *Combined analysis of Planck and SPTPol data favors the early dark energy models*, JCAP **08** (2020) 013, [[arXiv:2004.13046](#)].
- [29] A. Chudaykin, D. Gorbunov, and N. Nedelko, *Exploring an early dark energy solution to the Hubble tension with Planck and SPTPol data*, Phys. Rev. D **103** (2021), no. 4 043529, [[arXiv:2011.04682](#)].
- [30] J.-Q. Jiang and Y.-S. Piao, *Testing AdS early dark energy with Planck, SPTpol, and LSS data*, Phys. Rev. D **104** (2021), no. 10 103524, [[arXiv:2107.07128](#)].
- [31] J. C. Hill et al., *The Atacama Cosmology Telescope: Constraints on Pre-Recombination Early Dark Energy*, [arXiv:2109.04451](#).
- [32] V. Poulin, T. L. Smith, and A. Bartlett, *Dark energy at early times and ACT data: A larger Hubble constant without late-time priors*, Phys. Rev. D **104** (2021), no. 12 123550, [[arXiv:2109.06229](#)].
- [33] A. La Posta, T. Louis, X. Garrido, and J. C. Hill, *Constraints on Pre-Recombination Early Dark Energy from SPT-3G Public Data*, [arXiv:2112.10754](#).
- [34] G. Ye, B. Hu, and Y.-S. Piao, *Implication of the Hubble tension for the primordial Universe*

- in light of recent cosmological data*, Phys. Rev. D **104** (2021), no. 6 063510, [[arXiv:2103.09729](#)].
- [35] G. Ye and Y.-S. Piao, *T_0 censorship of early dark energy and AdS vacua*, Phys. Rev. D **102** (2020), no. 8 083523, [[arXiv:2008.10832](#)].
- [36] O. Akarsu, J. D. Barrow, L. A. Escamilla, and J. A. Vazquez, *Graduated dark energy: Observational hints of a spontaneous sign switch in the cosmological constant*, Phys. Rev. D **101** (2020), no. 6 063528, [[arXiv:1912.08751](#)].
- [37] L. Visinelli, S. Vagnozzi, and U. Danielsson, *Revisiting a negative cosmological constant from low-redshift data*, Symmetry **11** (2019), no. 8 1035, [[arXiv:1907.07953](#)].
- [38] K. Dutta, Ruchika, A. Roy, A. A. Sen, and M. M. Sheikh-Jabbari, *Beyond Λ CDM with low and high redshift data: implications for dark energy*, Gen. Rel. Grav. **52** (2020), no. 2 15, [[arXiv:1808.06623](#)].
- [39] R. Calderón, R. Gannouji, B. L’Huillier, and D. Polarski, *Negative cosmological constant in the dark sector?*, Phys. Rev. D **103** (2021), no. 2 023526, [[arXiv:2008.10237](#)].
- [40] Ruchika, K. Dutta, A. Mukherjee, and A. A. Sen, *Observational Constraints on Axion(s) with a Cosmological Constant*, [[arXiv:2005.08813](#)].
- [41] O. Akarsu, S. Kumar, E. Özülker, and J. A. Vazquez, *Relaxing cosmological tensions with a sign switching cosmological constant*, Phys. Rev. D **104** (2021), no. 12 123512, [[arXiv:2108.09239](#)].
- [42] A. A. Sen, S. A. Adil, and S. Sen, *Do cosmological observations allow a negative Λ ?*, [[arXiv:2112.10641](#)].
- [43] **Planck** Collaboration, N. Aghanim et al., *Planck 2018 results. VI. Cosmological parameters*, Astron. Astrophys. **641** (2020) A6, [[arXiv:1807.06209](#)]. [Erratum: Astron. Astrophys. 652, C4 (2021)].
- [44] **ACT** Collaboration, S. K. Choi et al., *The Atacama Cosmology Telescope: a measurement of the Cosmic Microwave Background power spectra at 98 and 150 GHz*, JCAP **12** (2020) 045, [[arXiv:2007.07289](#)].
- [45] **SPT-3G** Collaboration, L. Balkenhol et al., *Constraints on Λ CDM extensions from the SPT-3G 2018 EE and TE power spectra*, Phys. Rev. D **104** (2021), no. 8 083509, [[arXiv:2103.13618](#)].
- [46] F. Beutler, C. Blake, M. Colless, D. H. Jones, L. Staveley-Smith, L. Campbell, Q. Parker, W. Saunders, and F. Watson, *The 6dF Galaxy Survey: Baryon Acoustic Oscillations and the Local Hubble Constant*, Mon. Not. Roy. Astron. Soc. **416** (2011) 3017–3032, [[arXiv:1106.3366](#)].
- [47] A. J. Ross, L. Samushia, C. Howlett, W. J. Percival, A. Burden, and M. Manera, *The clustering of the SDSS DR7 main Galaxy sample – I. A 4 per cent distance measure at $z = 0.15$* , Mon. Not. Roy. Astron. Soc. **449** (2015), no. 1 835–847, [[arXiv:1409.3242](#)].
- [48] **BOSS** Collaboration, S. Alam et al., *The clustering of galaxies in the completed SDSS-III Baryon Oscillation Spectroscopic Survey: cosmological analysis of the DR12 galaxy sample*, Mon. Not. Roy. Astron. Soc. **470** (2017), no. 3 2617–2652, [[arXiv:1607.03155](#)].
- [49] **Pan-STARRS1** Collaboration, D. M. Scolnic et al., *The Complete Light-curve Sample of Spectroscopically Confirmed SNe Ia from Pan-STARRS1 and Cosmological Constraints from the Combined Pantheon Sample*, Astrophys. J. **859** (2018), no. 2 101, [[arXiv:1710.00845](#)].

- [50] J. Torrado and A. Lewis, *Cobaya: Code for Bayesian Analysis of hierarchical physical models*, JCAP **05** (2021) 057, [[arXiv:2005.05290](#)].
- [51] D. Blas, J. Lesgourgues, and T. Tram, *The Cosmic Linear Anisotropy Solving System (CLASS) II: Approximation schemes*, JCAP **07** (2011) 034, [[arXiv:1104.2933](#)].
- [52] A. Lewis, *GetDist: a Python package for analysing Monte Carlo samples*, [arXiv:1910.13970](#).
- [53] A. G. Riess et al., *A Comprehensive Measurement of the Local Value of the Hubble Constant with 1 km/s/Mpc Uncertainty from the Hubble Space Telescope and the SH0ES Team*, [arXiv:2112.04510](#).
- [54] A. La Posta, T. Louis, X. Garrido, and J. C. Hill, *Constraints on Pre-Recombination Early Dark Energy from SPT-3G Public Data*, [arXiv:2112.10754](#).
- [55] J. L. Bernal, L. Verde, and A. G. Riess, *The trouble with H_0* , JCAP **10** (2016) 019, [[arXiv:1607.05617](#)].
- [56] K. Aylor, M. Joy, L. Knox, M. Millea, S. Raghunathan, and W. L. K. Wu, *Sounds Discordant: Classical Distance Ladder & Λ CDM -based Determinations of the Cosmological Sound Horizon*, Astrophys. J. **874** (2019), no. 1 4, [[arXiv:1811.00537](#)].
- [57] E. Calabrese, A. Slosar, A. Melchiorri, G. F. Smoot, and O. Zahn, *Cosmic Microwave Weak lensing data as a test for the dark universe*, Phys. Rev. D **77** (2008) 123531, [[arXiv:0803.2309](#)].
- [58] H. Wang and Y.-S. Piao, *Testing dark energy after pre-recombination early dark energy*, [arXiv:2201.07079](#).
- [59] F. Niedermann and M. S. Sloth, *Resolving the Hubble tension with new early dark energy*, Phys. Rev. D **102** (2020), no. 6 063527, [[arXiv:2006.06686](#)].
- [60] S. Vagnozzi, *Consistency tests of Λ CDM from the early integrated Sachs-Wolfe effect: Implications for early-time new physics and the Hubble tension*, Phys. Rev. D **104** (2021), no. 6 063524, [[arXiv:2105.10425](#)].
- [61] G. Ye, J. Zhang, and Y.-S. Piao, *Resolving both H_0 and S_8 tensions with AdS early dark energy and ultralight axion*, [arXiv:2107.13391](#).
- [62] I. J. Allali, M. P. Hertzberg, and F. Rompineve, *Dark sector to restore cosmological concordance*, Phys. Rev. D **104** (2021), no. 8 L081303, [[arXiv:2104.12798](#)].
- [63] S. J. Clark, K. Vattis, J. Fan, and S. M. Koushiappas, *The H_0 and S_8 tensions necessitate early and late time changes to Λ CDM*, [arXiv:2110.09562](#).
- [64] H. N. Luu, *Axi-Higgs cosmology: Cosmic Microwave Background and cosmological tensions*, [arXiv:2111.01347](#).
- [65] B. S. Haridasu and M. Viel, *Late-time decaying dark matter: constraints and implications for the H_0 -tension*, Mon. Not. Roy. Astron. Soc. **497** (2020), no. 2 1757–1764, [[arXiv:2004.07709](#)].
- [66] E. Di Valentino, A. Melchiorri, O. Mena, and S. Vagnozzi, *Interacting dark energy in the early 2020s: A promising solution to the H_0 and cosmic shear tensions*, Phys. Dark Univ. **30** (2020) 100666, [[arXiv:1908.04281](#)].
- [67] W. Liu, L. A. Anchordoqui, E. Di Valentino, S. Pan, Y. Wu, and W. Yang, *Constraints from high-precision measurements of the cosmic microwave background: the case of disintegrating*

dark matter with Λ or dynamical dark energy, *JCAP* **02** (2022), no. 02 012, [[arXiv:2108.04188](#)].

- [68] L. Heisenberg, H. Villarrubia-Rojo, and J. Zosso, *Simultaneously solving the H_0 and σ_8 tensions with late dark energy*, [arXiv:2201.11623](#).
- [69] G. Ye and Y.-S. Piao, *Improved constraint on primordial gravitational waves in light of the Hubble tension and BICEP/Keck*, [arXiv:2202.10055](#).
- [70] F. Takahashi and W. Yin, *Cosmological implications of $n_s \approx 1$ in light of the Hubble tension*, [arXiv:2112.06710](#).
- [71] G. D'Amico, N. Kaloper, and A. Westphal, *Very Hairy Inflation*, [arXiv:2112.13861](#).
- [72] M. Mallaby-Kay et al., *The Atacama Cosmology Telescope: Summary of DR4 and DR5 Data Products and Data Access*, *Astrophys. J. Supp.* **255** (2021), no. 1 11, [[arXiv:2103.03154](#)].
- [73] T. L. Smith, M. Lucca, V. Poulin, G. F. Abellan, L. Balkenhol, K. Benabed, S. Galli, and R. Murgia, *Hints of Early Dark Energy in Planck, SPT, and ACT data: new physics or systematics?*, [arXiv:2202.09379](#).